RECEIVED BY OSTI JUL 25 1985
CONF-8505172--2

PARTITION OF CROSS SECTIONS IN ASYMMETRIC NUCLEUS-NUCLEUS REACTIONS AND THE ORIGIN OF FAST ALPHA PARTICLES

R. H. Siemssen†
Kernfysisch Versneller Instituut, 9747 Groningen, The Netherlands
and
Argonne National Laboratory, Argonne, IL. 60439, U.S.A.

CONF-8505172--2

DE85 014989

ABSTRACT

To investigate the mechansim of asymmetric nucleus-nucleus reactions from the Coulomb barrier to intermediate energies the $^{14}N + ^{159}Tb$ reaction was studied at five bombarding energies between 8 and 23 MeV/u via particle-particle correlations (at selected energies) and particle KX-ray coincidences to identify the specific reaction channels. With the KX-ray method partial cross sections for projectile-like fragments (PLF) as a function of the atomic number (Z_{res}) of the residual nucleus can be determined. The charge balance yields the "missing charge" $dZ = Z_{proj} + Z_{targ} - Z_{PLF} - Z_{TLF}$ that indicates whether, in addition to the PLF, other charged particles are emitted. A large fraction of the inclusive cross sections is found to originate from such channels with two or more fragments in the exit channel, and this fraction increases as the PLF is further removed in mass from the incident projectile, and with increasing bombarding energy. From the particle-particle correlation studies it is found that sequential decays of PLF's are dominant. "Non-sequential" processes, if present, are associated with inelastic reactions involving excitations of both projectile and target. The bulk of the large alpha-particle cross section at small angles is found to be associated with channels in which, in addition to the alpha particle, only nucleons amd other alpha particles are emitted. From γ-ray multiplicity measurements and from the broad distribution of the strength with Z_{res} it is concluded that these alpha particles originate from inelastic (damped) processes.

I. INTRODUCTION

During the past years much effort has gone into the study of the evolution of the mechanism of heavy ion reactions from the Coulomb barrier to intermediate energies. For reactions with light heavy ions to which this talk is restricted some of the questions of continuing interest are the role of pre-equilibrium processes and related, the large abundance of fast alpha particles and nucleons at small angles, the properties of incomplete fusion reactions, and the appearent differences between reactions with light heavy ions on one hand and those involving massive nuclei on the other. More generally the interest is in exploring the transition from an energy domain in which the reactions are governed by mean field effects to a region where collisions between individual nucleons of the colliding nuclei become important.

---

†Work done in collaboration with:

G. J. Balster, P. D. Bond, P. C. N. Crouzen, P. B. Goldhoorn, Han Shukui, Z. Sujkowski and H. W. Wilschut

From an experimental view point the reactions of interest are characterized by an increasing complexity with bombarding energy as more and more channels open and as also "non-binary" processes become energetically possible that may lead to a large number of fragments in the final state. Various experimental techniques are being applied that range from particle-particle correlation studies (1), particle-γ (2) and particle-KX-ray (3) coincidence measurements to identify the reaction channels to 4 π neutron detection (4) and measurements with a "plastic box" (5). A difficulty often encountered is the fact, that short of employing a 4 π detection in which all reaction products are accounted for, the results might be biased by the experimental method and by looking at just a few channels.

In my talk I will report on a continuing study of asymmetric nucleus-nucleus colllisions in which we have been involved at Groningen during the past years. Rather than to investigate different target-projectile combinations the approach taken by us was to mainly concentrate on one nucleus-nucleus system ($^{14}N + {}^{159}Tb$) with the goal to obtain for it an as complete as possible set of data that might then serve as a benchmark for further theoretical studies. Measurements have been done at five different energies between 8 and 23 MeV/u and have involved, aside of singles data particle-particle correlation studies at selected energies (6), particle-γ at 10 MeV/u (7) and particle-KX-ray coincidence experiments (8), and γ-ray multiplicity measurements. From the KX-ray coincidence measurements a rather unique set of data has been obtained from a which a global picture of the reaction mechanism of light heavy ions at energies < 20 MeV/u is emerging.

II. INCLUSIVE DATA

Inclusive particle spectra (not shown) measured in the vicinity of the grazing angle peak in energy at approximately beam velocity at an optimum Q-value in agreement with the Siemens (9) prediction including a dissipative term (7). The mass flow is almost exclusively from the projectile to the target. Angular distributions for particles ranging from ^{4}He to ^{16}O are strongly forward peaked and fall off with angle almost exponentially. Energy spectra and angular distributions are typical of a quasi-elastic process. At larger angles, however, indications are also found for a (weak) deep-inelastic component. From particle-γ coincidence measurements it was deduced (7) that only 40%-60% of the inclusive cross sections could be accounted for by incomplete fusion with the projectile-like fragment emitted in a particle stable state.

III. PARTICLE-PARTICLE CORRELATION STUDIES

Particle-particle correlation studies to explore the reaction mechanism of asymmetric nucleus-nucleus reactions are widely employed to trace down the origin of fast alpha particles and nucleons with the goal to identify pre-equilibrium phenomena and to study the importance of breakup and fragmentation. Extensive and rather up-to-date references can be found in the papers of Bhowmik et al.(6) which deals with the $^{14}N + {}^{159}Tb$ reaction and from which most of the results presented in this section are taken, and by Gonthier et al.(10).

In fig.1 HI-alpha double differential cross sections measured for the $^{14}N + ^{159}Tb$ system at 168 MeV are shown for ^{10}Be, ^{10}B and ^{11}B. Very similar data were obtained for ^{4}He, ^{6}Li, ^{7}Li and ^{9}Be. In these measurements the HI detector was positioned at 20° and the alpha detector was moved in the reaction plane. The coincidence yield is enhanced if the two detectors are close together as a consequence of kinematic focusing following sequential decay of projectile-like fragments (PLF's). The correlation has a Gaussian-like shape and is slightly skewed if the detectors are placed at opposite sides of the beam. The very small cross sections at large angles indicate that alpha decays from the target-like fragment (TLF) are relatively unimportant.

Unambiguous evidence for sequential decay of PLF's can be obtained from the relative energy spectra of the two fragments in their respective center-of-mass frame. This is shown in fig.2 for $^{14,15}N$ and ^{10}B decaying into $^{10,11}B$ and $^{6}Li + \alpha$ (11). The relative energy spectra (top) are seen to exhibit sharp peaks that correspond to known particle-unstable states in the parent PLFs. The observed widths of these peaks of approximately 100 keV are determined by the experimental resolution. Their narrowness implies that the decay times are long with respect to the reaction time. Formation and decay of the fragments are thus well separated in space and time. Also shown in these figures (bottom row) are the total energy spectra $E_{HI} + E_{\alpha}$ for the respective systems. The total energy spectra resemble those of the parent PLF's and peak around the optimum Q-values for quasi-elastic processes.

For $^{14,15}N$ as parent most of the strength is concentrated near the ground state of the target-like residual nucleus. The particle decaying states seen in ^{14}N and ^{15}N are those that would be excited in inelastic scattering, respectively one-neutron transfer. All these observations point towards a (direct) quasi-elastic excitation of at least those PLF's that are not too far removed in mass from the incident projectile. For ^{10}B as parent PLF the residual nucleus is highly excited as would be the case e.g. in an incomplete fusion reaction with ^{10}B as ejectile.

With a knowledge of the relative energy spectra, of the angular distributions of the parent PLF, and of the two fragments in their center-of-mass frame the particle-particle correlations can be computed (12). The results of such calculations made with the assumption of an isotropic angular distribution of the two fragments in their c.m. frame are shown in fig. 3 as solid curves together with the corresponding data. Whereas these calculations do quite well for the angular range in which the two detectors are close to each other, they underpredict the cross section at the far side. Such an underprediction has been found consistently by several authors (10,13) and has been attributed to "non-sequential", pre-equilibrium alpha particles.

In our previous publications (6,11) we had related the possible non-sequential component to an "uncorrelated component" that is approximately symmetric about the beam axis and that was initially proposed by the Birmingham group (14) on the basis of their study of the $^{14}N + ^{58}Ni$ reaction at 148 MeV. In a recent reexamination of this reaction (15) we could not substantiate their findings and instead observe strong sequential decays that contradict the previous conclusions and thus eliminate the basis for the uncorrelated component.

Of interest in conjunction with the foregoing discussion on the possible presence of a "non-sequential" component is the observation that the $^{11}B + \alpha$ angular correlation data obtained by gating on the quasi-elastic peak is much narrower (fig.1, data labeled Q.E.) and in better agreement with a purely sequential process than without a gate on the total energy. This results indicates that the "non-sequential" component if present is associated with inelastic events.

It is furthermore of interest to examine relative energy spectra from particle-particle correlation measurements for different inelasticities. This is done in fig.4 for the reaction $^{16}O + ^{208}Pb$ at 160 MeV (16) leading to $^{12}C + \alpha$. On the top of the figure the Q-value (total energy) spectrum is shown. With the gate on the quasi-elastic peak the relative energy spectrum exhibits sharp peaks corresponding to known states in ^{16}O with almost no background, whereas with the gate set to select inelastic events a large background is seen. Very similar observations were made by Rae et al. (17). Particle decays of ^{16}O leading to the first excited state of ^{12}C account for at least some of the background.

An alternative explanation for the observed anomalies attributed to the emission of pre-equilibrium alpha particles would be the decay of the parent PLF's into more than two fragments. As shown in section V such decay channels can be rather strong and moreover the importance of these processes will increase with inelasticity. We are presently investigating whether these can explain both the additional coincidence cross sections when the two detectors are far apart as well as the background in the relative energy spectra.

In summary there is clear evidence for sequential decays both from particle-particle correlation data and from relative energy spectra. The excitation of the parents appears to proceed via a quasi-elastic process for PLF's close in mass to the incident projectile. A "non-sequential" component, if present, is found to be related to inelastic events involving excitations of both target and projectile. This "non-sequential" component might originate from pre-equilibrium alpha particles but alternatively might also reflect the decays of the parent PLF's into more than two fragments.

IV. THE KX-RAY METHOD

A powerful method in the study of asymmetric nucleus-nucleus reactions is the measurement of coincidences between PLF's and γ-rays to identify the residual nucleus and thus the reaction channel. Following the pioneering work of Inamura et al.(2) this method has been applied in many laboratories and also to the investigation of the $^{14}N + ^{159}Tb$ reaction at 140 MeV for which cross sections were obtained for a large number of incomplete fusion channels (7). A drawback of the method is that the analysis of the data is very cumbersome especially for odd-A residual nuclei and that the γ-ray spectra become prohibitively complex with increasing energy.

An alternative method extensively explored by us during the past years is the measurement of particle-KX-ray coincidences (3) to identify the residual nuclei. The measurement of characteristic X-rays was already employed in the sixties for the investigation of fission inluding coincidence measurements between fission products and KX-rays (18). Inclusive KX-ray measurements following heavy ion reactions more recently were performed by Karwoski et al. (19) and Ernst et al. (20).

Since the KX-ray angular distribution is isotropic cross sections can be readily obtained from coincidence measurements at one angle if the KX-ray multiplicities are known. These in general will depend on the way the residual nucleus is excited and on its structure. Studies of KX-ray multiplicities in the rare earth region (21,22) in which the residual nuclei are good rotors indicate, however, that the multiplicities in this mass region are rather insensitive to the specific reaction and that multiplicities obtained by averaging over several isotopes show a systematic trend with an odd-even staggering depending on the atomic number of the residual nucleus. This observation suggests that it might be possible to work with average multiplicities instead of having to determine the multiplicities individually for every residual nucleus.

We indeed find for the $^{14}N + ^{159}Tb$ reaction that we can consistently describe a large body of data measured at different energies by employing average KX-ray multiplicities (0.6 for Z_{even} and 1.2 for Z_{odd}). With these we obtain the inclusive cross sections as the sum of the exclusive particle-KX-ray cross sections within about 20%. This consistent description of a large body of data gives us considerable confidence in the KX-ray method to obtain both relative and absolute cross sections.

KX-ray spectra from the $^{14}N + ^{197}Au$ reaction at 168 MeV (3) are presented in fig.5. In the top the inclusive spectrum is shown in which the atomic X-rays from inner shell ionization dominate. Below are the spectra obtained in coincidence with ^{11}B, ^{7}Li and alpha particles. Noteworthy is the observation that for ^{11}B the lines are those expected for incomplete fusion (capture of Z=2 by the target) whereas for ^{7}Li in addition to the lines from incomplete fusion (Z=4 charge transfer) also those for Z = 2 transfer are seen. The latter point to a process in which the PLF is an excited ^{11}B that subsequently decays into ^{7}Li and an alpha particle, the contributions from alpha decay of the TLF being unimportant as was independently verified. From the relative strengths of the transitions leading to the same Z_{res} the probabilities for emission of PLF's in particle unstable states can be deduced from the KX-ray coincidence data. These were found (8) to be in good agreement with those deduced from the particle-particle correlation measurements. For the alpha particles the KX-ray spectrum of fig. 5 is seen to be very complex thus indicating contributions from many different channels.

V. PARTIAL CROSS SECTION DATA

Particle-KX-ray coincidence data for the $^{14}N + ^{159}Tb$ system were obtained at 115, 140, 168, 236 and 308 MeV. We will concentrate here mainly on the 236 MeV data. As an example of the type and quality of data that were obtained partial cross sections for ^{7}Li, ^{9}Be, ^{11}B and ^{12}C measured at 140 and 236 MeV are plotted in fig.6 versus the atomic number (Z_{res}) of the residual nuclei. The right most bars correspond to incomplete fusion channels for which the "missing charge"

$$dZ = Z_{PROJ} + Z_{TARG} - Z_{PLF} - Z_{TLF}$$

is zero. Especially for the lighter ejectiles a large fraction of the cross sections is found in channels with missing charge $dZ \neq 0$, and this fraction is seen to increase with bombarding energy. A very similar result was obtained by Stokstad et al. with the plastic box (5). From coincidence measurements with alpha particles and protons at backwards angles it can be concluded that only a small fraction of the missing charge can be attributed to charged particle evaporation from the TLF. The strength in these channels must therefore be attributed to (sequential) decays of excited PLF's or to pre-equilibrium emission of light particles as discussed in the previous section.

In fig. 7 partial alpha particle cross sections obtained at three different energies are plotted versus Z_{res}. It is interesting to note that incomplete fusion is the strongest channel at 115 MeV. Next in importance are the channels with two (^{8}Be) and three alpha particles (^{12}C*) in the final state which at this energy might also be attributed to incomplete fusion. In contrast the incomplete fusion channel with one alpha particle out is extremely weak 236 MeV though some of its strength will be depleted by charged particle evaporation and fission. Channels with missing charge unequal zero clearly dominate the alpha particle spectrum at 236 MeV, whereby it is interesting to note that the cross section for Z_{res} = 66 still protrudes, probably reflecting the low threshold in carbon for its desintegration into three alpha particles.

Table I contains the cross section matrix for the ^{14}N + ^{159}Tb reaction at 236 MeV and 20°. The columns correspond to the atomic numbers of the residual nuclei and the rows to different PLF's. Since the KX-ray method cannot identify neutron decays cross sections for different isotopes of the PLF have been combined. Adding the cross sections in one row should yield the inclusive cross section for a given PLF as is indeed the case within about 20%. The summed cross sections as well as the measured inclusive cross sections are listed in Table I in the last two columns. If one assumes that PLF's with missing charge unequal zero originate from sequential nucleon or alpha decay of projectile-like fragments cross sections for the production of the parent PLF's in a particle unstable state can also be obtained from table I by adding the corresponding numbers within one column. In fig. 8 we show differential cross sections for the production of the different PLF's in a particle stable (solid bars), respectively particle unstable state (open bars) together with the measured inclusive cross sections (shaded bars). To avoid double counting only cross sections for PLF's with Z > 2 have been added to obtain the cross sections of the primary fragments. The cross sections of primary PLF's in the top of fig. 8 are seen to drop off steeply as the PLF is further removed in charge (mass) from the incident projectile. This steep fall off is characteristic of a quasi-elastic process.

VI. GAMMA RAY MULTIPLICITIES

In parallel to the KX-ray measurements γ-ray multiplicities were obtained by requiring triple coincidences between PLF's, KX-rays and γ-rays. The results of these measurements are shown in fig. 9. In the upper half multiplicities for different residual nuclei are plotted versus missing charge. For Tb (Z_{res} = 65) e.g. missing charges of one to five correspond to the detection of C, B, Be, Li and He, respectively. A missing charge of 5 thus implies that in addition to the detected alpha particle either two alpha particles and a proton, an alpha particle and a lithium, or a boron nucleus are emitted.

As is seen from fig. 9 the γ-ray multiplicity and thus the inelasticity increases with missing charge. This is most dramatic for terbium for which the multiplicity is 3 with a nitrogen emitted in a particle stable state and it is 11 if an alpha particle is detected. (From a parallel measurement at large angles it can be concluded that the bulk of these forward angle alpha particles do not originate from the TLF). The large γ-ray multiplicity for alpha particles implies a strong excitation of the TLF that is the more remarkable as with terbium both as target and as residual nucleus the mass transfer to the residual nucleus is small involving at best a few neutrons.

From the foregoing it can be concluded that increasingly more inelastic processes in which both target and projectile are excited are required to disintegrate the PLF into more than two fragments. This is in contrast to the observation in sect. III in which the excitation of nitrogen into alpha decaying states could be explained by (one-step) quasi-elastic processes.

In the lower half of fig. 9 γ-ray multiplicities for different PLF's are plotted versus missing charge. For a given PLF the multiplicities are largest for zero missing charge, and the multiplicities also increase as the mass of the PLF decreases. Both results can be readily understood in the framework of incomplete fusion since the angular momentum imparted in these reactions to the target is proportional to the mass of the fragment that is captured. With a missing charge of zero the lighter the detected PLF the more massive the captured fragment. For a missing charge unequal zero the detected PLF on the other hand is not the primary fragment.

VII. ORIGIN OF FAST ALPHA PARTICLES

In fig. 7 the large abundance of alpha particles at 20° was shown. From measurements at backward angles it can be deduced that only a small fraction of these (< 5%) can be accounted for by evaporation from the TLF. From the cross section matrix in Table I the yield of alpha particles that are not in coincidence with a PLF with $Z > 2$ can be deduced. These cross sections in fact account for the bulk of the alpha particle yield at forward angles. They are shown as bargraphs in the lower half of fig. 8 whereby the alpha particle multiplicities have been divided out. The labeling on the abscissa gives the number of alpha particles and protons emitted per event for a given Z_{res}. The assumption made is that it is favourable to emit an alpha particle rather than two protons and that a missing charge of three thus corresponds to an alpha particle and a proton.

In striking contrast to the steep fall-off of the yield of primary fragments with mass transfer typical of a quasi-elastic process the yield of alpha particles shows a much broader distribution as a function of Z_{res} (fig. 8). This observation suggests that the alpha particles do not originate from a quasi-elastic but from a more inelastic process instead for which the mass distributions are known to be wider. The conjucture of an inelastic (damped) process is also supported by the γ-ray multiplicity measurements that were discussed in section VI and that have shown the inelasticity to increase with missing charge. These measurements indicate that the bulk of the alpha particles and nucleons does not originate from elastic breakup.

Results very similar to those derived from the γ-ray multiplicity measurements were obtained by Fuchs et al. (23) who measured neutron multiplicities in coincidence with alpha particles without, however, specifying the reaction channel. As shown in fig. 10 in which the neutron multiplicities are plotted these authors identify their components, one due to evaporation from the TLF (marked EV) which is relatively unimportant at forward angles, one with a low neutron multiplicity that the authors ascribe to projectile breakup (BU) and that is probably related to the sequential decays discussed in Sect. III and a third component with a high neutron multiplicity labeled non-equilibrium (NE). The latter we associate with the bulk of the alpha particles that are not in coincidence with PLF's with Z > 2.

From the foregoing it is tempting to associate the bulk of the alpha particles with deep-inelastic processes though from the energies of the alpha particles it must be concluded that these do not originate from a process in which all kinetic energy has been dissipated. A possible mechanism might be that the alpha particles and nucleons are produced in the initial step of energy dissipation in the deep-inelastic process. On the other hand the large yields for two, respectively three alpha particles at Z_{res} = 68 and 66 especially at the lower incident energies (fig. 7) seem to reflect the low alpha particle thresholds in ^{8}Be and ^{12}C. At present we cannot say whether the alpha particles and nucleons are the products of a sequential decay chain or whether they are produced in the initial phase of the reaction.

It is also of interest to investigate whether there is a relation between the present observation on the production of alpha particles and recent results from GANIL (24-26). In these studies in addition to a quasi-elastic component fragmentation with a broad mass distribution ranging from the projectile to very light fragments is found together with a more relaxed component that persists even at intermediate energies. If fragmentation is the source of the alpha particles the present results would indicate that there is energy damping associated with these processes leading to an excitation of both projectile and target.

One may finally ask why not to ascribe the bulk of the alpha particles to more conventional pre-equilibrium processes based e.g. on exciton models (27). From these models, however, one would expect many more nucleons to be emitted than alpha particles in contrast to observation.

SUMMARY

Employing the KX-ray method it was possible to obtain partial (exclusive) cross sections for PLF's ranging from alpha particles to carbon for different atomic numbers of the residual nuclei. Inclusive cross sections can be fully accounted for by the measured exclusive cross sections. The emission of charged (light) particles in addition to the PLF can be deduced from the missing charge. Results obtained with the KX-ray method are very similar to those from measurements with the plastic box by Stokstad et al.(5). Particle-particle correlation studies show sequential decays of PLF's to be important. "Non-sequential" processes, if present, are associated with inelastic (damped) reactions involving excitation of both projectile and target. Decays of PLF's into more than two fragments might, however, account for some of the observed deviations from sequential decay. From the KX-ray data cross sections for the production of primary fragments in a particle stable, respectively particle unstable state can be deduced.

Production cross sections of primary fragments fall off steeply as the PLF is removed in mass from the incident projectile in qualitative agreement with expectations for quasielastic processes. For the lightest fragments only a small fraction of the inclusive cross section is due to processes in which the detected PLF is the primary fragment. The bulk of the large cross section for the production of alpha particles at small angles is associated with processes in which the detected alpha partice is emitted together with nucleons and alpha particles but not with PLF's with $Z > 2$, thus excluding sequential decay processes of PLF's into a heavy ion and an alpha particle as the main source of these alpha particles.

Production cross sections for the alpha particles as a function of Z_{res} show a rather flat distribution indicative of a more damped process. This pictue is also supported by measurements of neutron- (23) and γ-ray multiplicities. It is tempting to relate the bulk of the alpha particles to (deep)-inelastic processes though the energy of the alpha particles excludes sequential decays from PLF's following complete energy relaxation. If fragmentation processes are the origin of the alpha particles the observed features would indicate some energy damping in these reactions reminiscent perhaps of the initial phase of deep-inelastic reactions.

The help of G. J. Balster in the preparation of this manuscript is gratefully acknowledged. This work was performed as part of the research program of the Stichting voor Fundamenteel Onderzoek der Materie (FOM) with the financial support of the Nederlandse Organisatie voor Zuiver-Wetenschappelijk Onderzoek (ZWO) and the U. S. Department of Energy under Contract W-31-109-Eng-38.

FIGURE CAPTIONS

Fig. 1: HI-alpha coincidence data from the $^{14}N + ^{159}Tb$ reaction at 168 MeV. The vertical dashed line indicates the angle of the HI-detector. The curves through the data points are to guide the eye.

Fig. 2: Relative (top) and total energy spectra (bottom) from HI-alpha coincidence data from the $^{14}N + ^{159}Tb$ reaction at 140 MeV.

Fig. 3: Comparison of the HI-alpha coincidence data at 168 MeV with calculated angular correlations.

Fig. 4: Total (top) and relative energy spectra (below) for $^{12}C + \alpha$ coincidences in the $^{16}O + ^{208}Pb$ reaction at 160 MeV obtained by setting different gates on the total energy.

Fig. 5: KX-ray spectra obtained for the $^{14}N + ^{197}Au$ reaction at 168 MeV.

Fig. 6: Partial cross sections obtained for selected PLF's via particle - KX-ray coincidences in the $^{14}N + ^{159}Tb$ reaction at 20° and at 140 and 236 MeV, respectively.

Fig. 7: Partial cross sections for alpha particles measured at three different energies.

Fig. 8: Cross sections for the production of primary fragments in the ^{14}N + ^{159}Tb reaction at 236 MeV and 20° (a) in a particle stable state (solid bars), respectively particle unstable state (open bars). Also shown are the inclusive cross sections (shaded bars). In the lower half (b) cross sections for alpha particles that are not accompanied by an heavy ion are plotted versus the atomic number of the residual nucleus. The cross sections have been corrected for alpha particle multiplicities.

Fig. 9: γ-ray multiplicities measured at 236 MeV for the ^{14}N + ^{159}Tb reaction plotted versus missing charge. In the upper half multiplicity data of reactions leading to the same Z_{res} are grouped together, in the lower half those associated with the same PLF.

Fig. 10: Neutron multiplicities measured in coincidence with alpha particles in the ^{20}Ne + ^{197}Au reaction (23) at two different energies. Indicated in the figure as hatched areas are the contributions of alpha particles originating from breakup (sequential decays), from evaporation from the TLF and of "non-equilibrium" alpha particles.

REFERENCES

1. C. K. Gelbke et al., Phys. Lett. 71B (1977) 83; H. Ho et al., Z. Phys. A283 (1977) 235; J. W. Harris et al., Phys. Rev. Lett. 38 (1977) 1460.

2. T. Inamura, M. Ishihara, T. Fukuda, T. Shimoda and H. Hiruta, Phys. Lett. B68 (1977) 51.

3. H. W. Wilschut, R. K. Bhowmik, P. B. Goldhoorn, J. F. W. Jansen, R. H. Siemssen, K. Siwek-Wilczynska, Z. Sujkowski and J. Wilczynski, Phys. Lett. 123B (1983) 173.

4. U. Jahnke, G. Ingold, H. Homeyer, M. Buergel, Ch. Egelhaf, H. Fuchs, D. Hilscher, Phys. Rev. Lett. 50 (1983) 1246.

5. R. G. Stokstad et al., in Proc. Int. Symp. Heavy Ion Physics, Mt. Fuji, Aug., 1984, Part II, p.71.

6. R. D. Bhowmik, J. van Driel, R. H. Siemssen, G. J. Balster, P. B. Goldhoorn, S. Gongrijp, Y. Iwasaki, R. V. F. Janssens, H. Sakai, K. Siwek-Wilczynska, W. A. Sterrenburg and J. Wilczynski, Nucl.Phys. A390 (1982) 117.

7. J. Wilczynski, K. Siwek-Wilczynska, J. van Driel, S. Gongrijp, D. C. J. M. Hageman, R. V. F. Janssens, J. Lukasiak, R. H. Siemssen and S. Y. van der Werf, Phys. Rev. Lett. 45 (1980) 606 & Nucl. Phys. A373 (1982) 109.

8. G. J. Balster, R. K. Bhomik, P. B. Goldhoorn, R. H. Siemssen, Z. Sujkowski, and H. W. Wilschut, Phys. Lett. 143B (1984) 79.

9. P. J. Siemens, J. P. Bondorf, D. H. E. Gross and F. Dickmann, Phys.Lett. 36B (1971) 24.

10. P. L. Gonthier, H. Ho, M. N. Namboodiri, J. B. Natowitz, L. Adler, S. Simon, K. Hagel, S. Kniffen and A. Khodai, Nucl. Phys. A411 (1983) 289.

11. J. van Driel, S. Gongrijp, R. V. F. Janssens, R. H. Siemssen, K. S. Siwek-Wilczynska and J. Wilczynski, Phys. Lett. 98B (1981) 351.

12. G. R. Young et al., Phys. Rev. Lett. 45 (1980) 1389.

13. H. Ho et al., Phys. Rev. C27 (1983) 584.

14. R. K. Bhowmik, E. C. Pollaco, N. E. Sanderson, J. B. A. England and G. C. Morrison, Phys. Rev. Lett. 43 (1979) 619 & Nucl. Phys. A363 (1981) 516.

15. P. B. Goldhoorn, G. J. Balster, H. J. Koeslag, R. J. de Meijer, R. H. Siemssen, Z. Sujkowski, and H. W. Wilschut, Phys. Lett. 142 (1984) 14.

16. R. K. Bhowmik, S. Gongrijp, R. Kamermans, R. H. Siemssen and J. Wilczynski, KVI Ann. Rep. 1980, p.68.

17. W. D. M. Rae, A. J. Cole, B. G. Harvey and R. G. Stokstad, Phys.Rev C30 (1984) 158, and Rae et al. Phys. Lett. 105B (1981) 417.

18. W. Reisdorf, J. P. Unik, H. C. Griffin and L. E. Glendenin, Nucl. Phys. A177 (1971) 337, and references therein.

19. H. J. Karwowski, S. E. Vigdor, W. W. Jacobs, S. Kailas, P. P. Singh, T. G. Throwe, T. E. Ward, D. L. Wark and J. Wiggins, Phys. Rev. C25 (1982) 1355 & Phys. Rev. Lett. 42 (1979) 1732.

20. M. Ernst, W. Henning, C. N. Davids, W. S. Freeman, T. J. Humanic, F. W. Prosser, and R. A. Racca, Phys. Rev. C29 (1984) 464 & Phys. Lett. 119B (1982) 307.

21. D. Chmielewska, Z. Sujkowski, R. V. F. Janssens and M. J. A. de Voigt, Nucl. Phys. A366 (1981) 142.

22. Z. Sujkowski, G. J. Balster, D. Chmielewska and H. W. Wilschut, Phys. Lett. 133B (1983) 53.

23. H. Fuchs, M. Buergel, H. Homeyer, G. Ingold, U. Jahnke and G. Thoma, Phys. Rev. C31 (1985) 465.

24. V. Borrel, D. Guerreau, J. Galin, B. Gatty, D. Jacquet and X. Tarrago, Z. Phys. A314 (1983) 191.

25. B. Borderie, M. F. Rivet, C. Cabot, D. Fabris, D. Gardes, H. Gauvin, F. Hanappe and J. Peter, Z. Phys. A318 (1984) 315.

26. F. Rami, J. P. Coffin, G. Guillaume, B. Heusch, P. Wagner, A. Fahli and P. Fintz, Z. Phys. A318 (1984) 239.

27. M. Blann, Phys. Rev. C31 (1985) 1245.

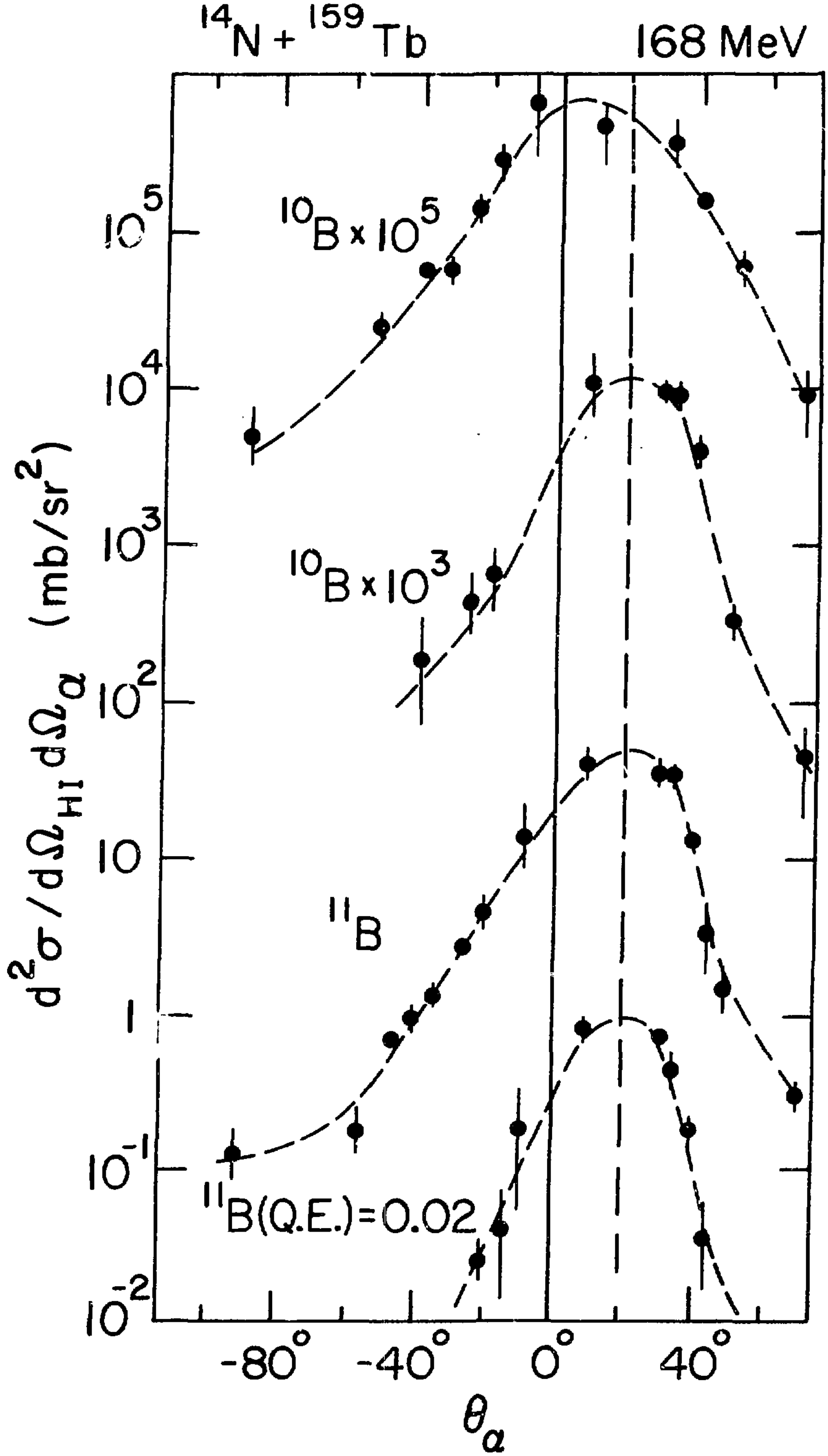

14N + 159Tb
168 MeV
10B x 10^5
10B x 10^3
11B
11B(Q.E.)=0.02
10^5
10^4
10^3
10^2
10
1
10^-1
10^-2
d2σ/dΩHI dΩα (mb/sr2)
-80°
-40°
0°
40°
θα

Fig. 1

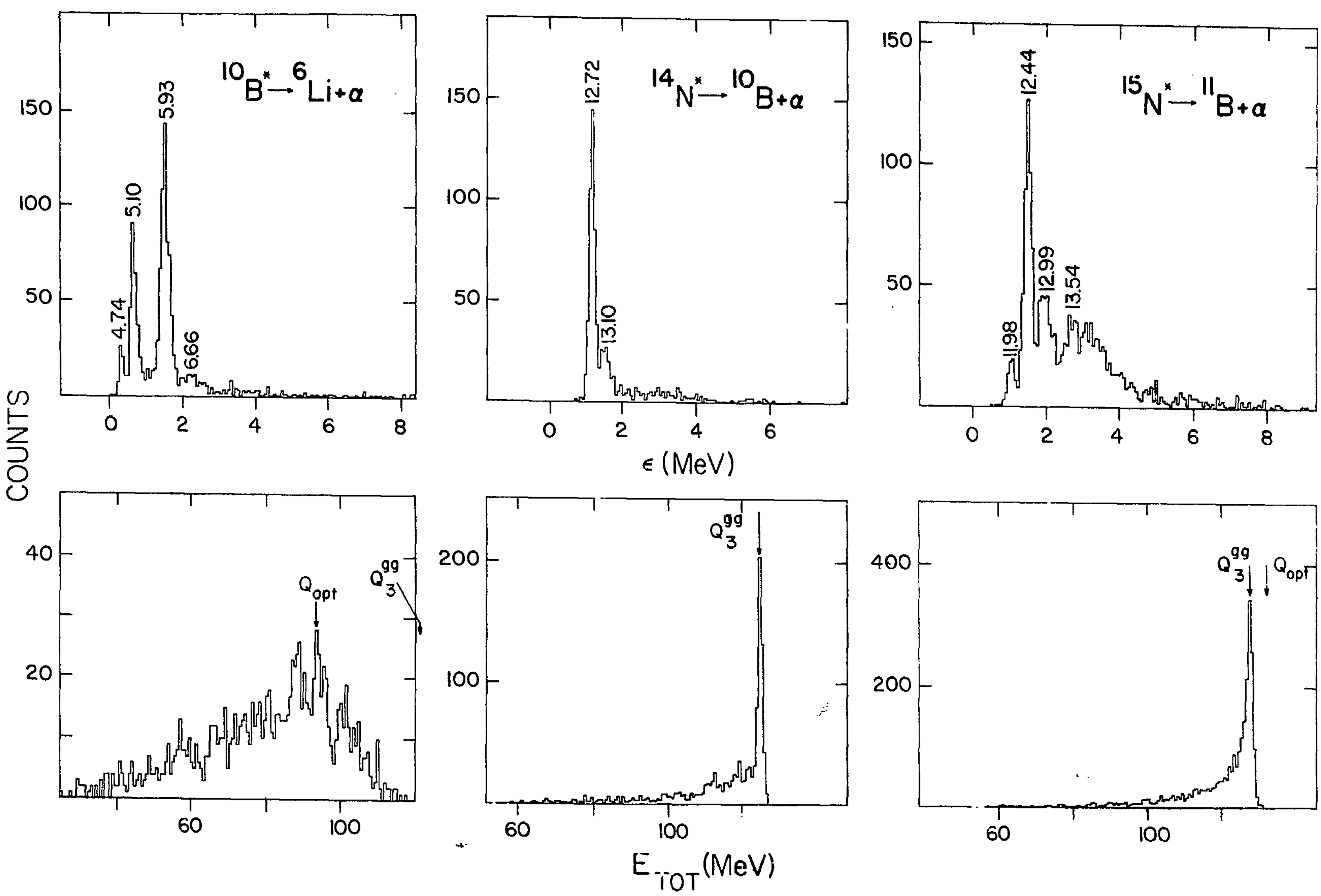

COUNTS
10B* → 6Li+α
14N* → 10B+α
15N* → 11B+α
4.74
5.10
5.93
6.66
12.72
13.10
11.98
12.44
12.99
13.54
ε (MeV)
Qopt
Q3gg
E TOT (MeV)

Fig. 2

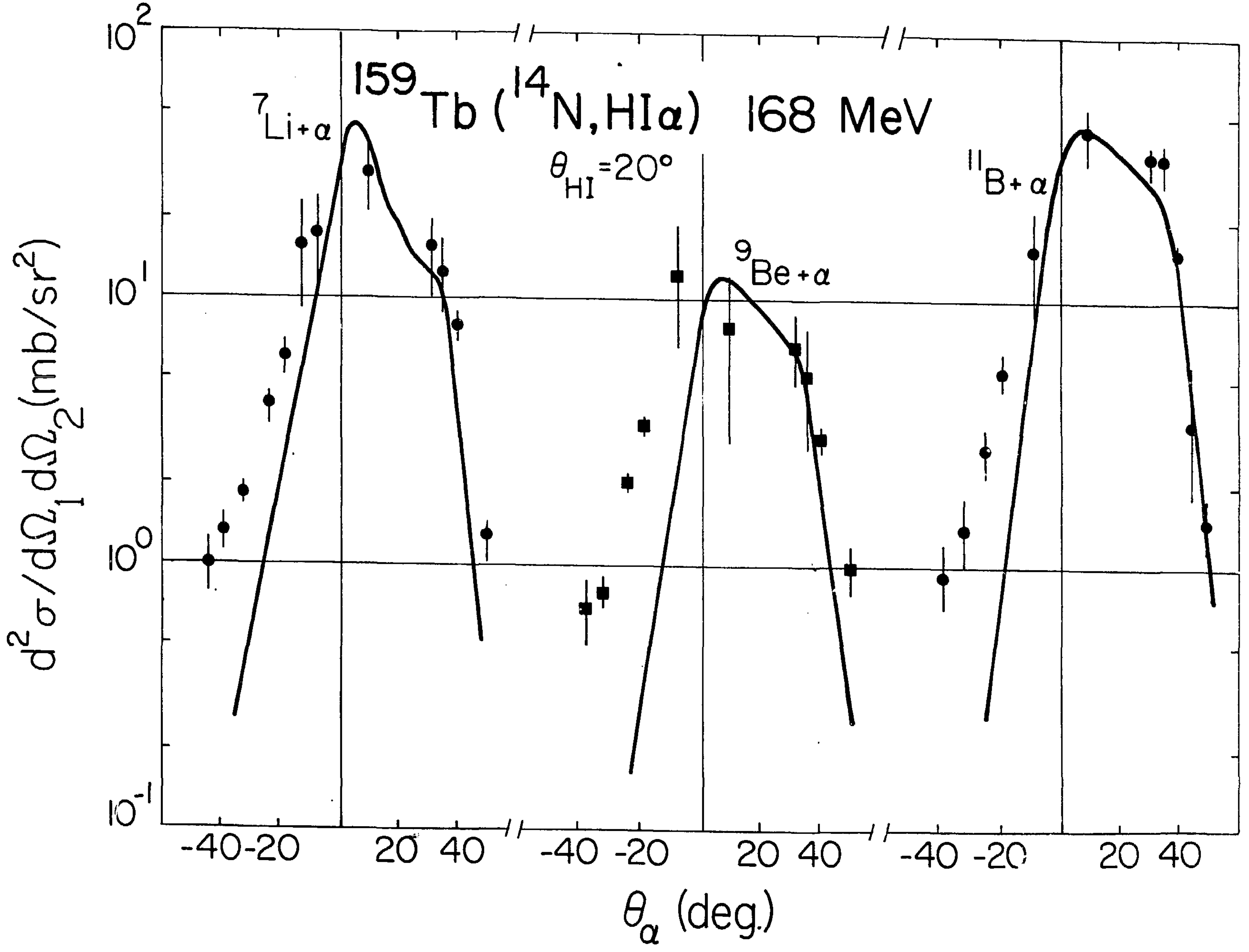

^{159}Tb (^{14}N,HIα) 168 MeV
θ_{HI}=20°
^{7}Li+α
^{9}Be+α
^{11}B+α
$d^2\sigma/d\Omega_1 d\Omega_2$(mb/sr^2)
θ_α (deg.)

Fig. 3

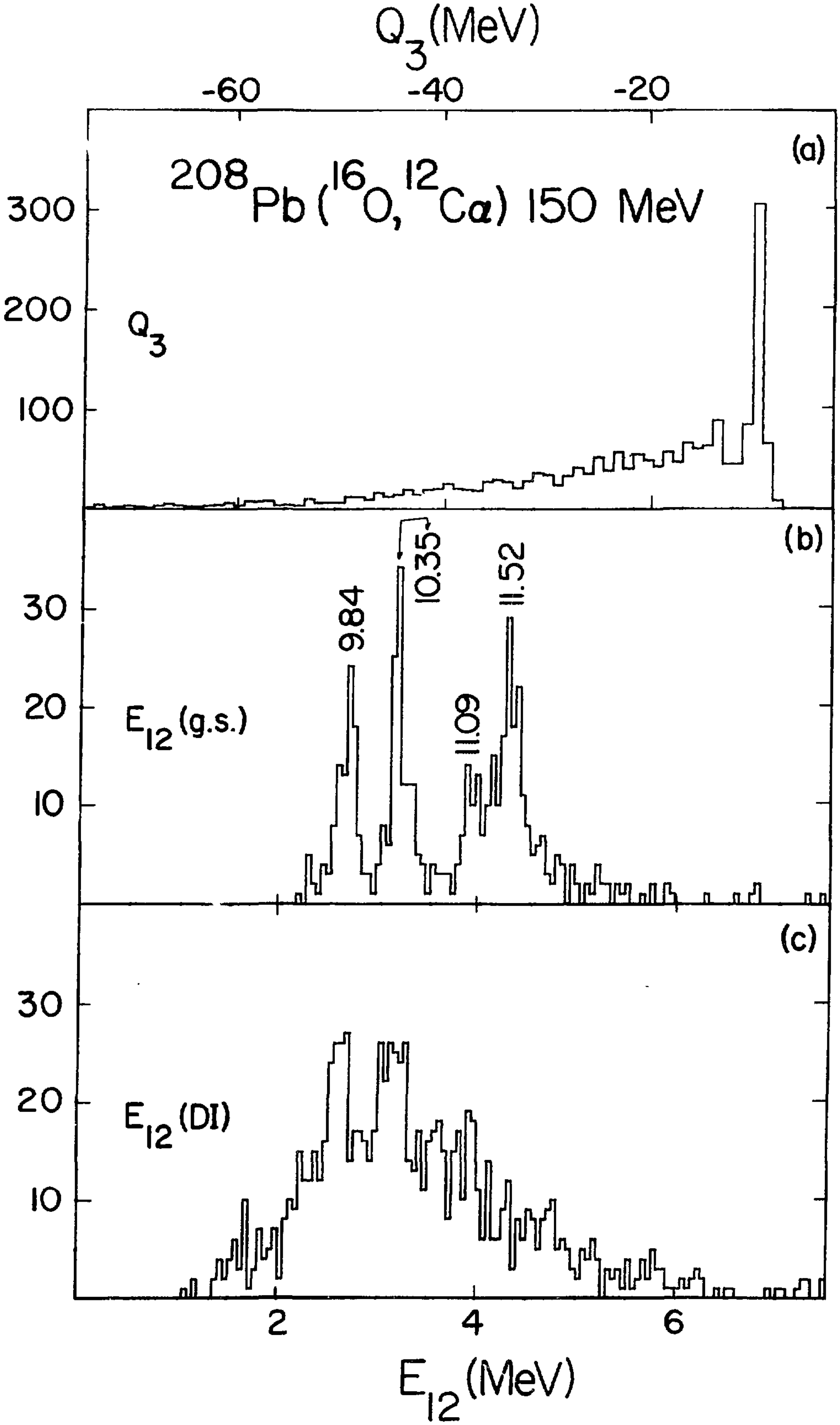
Q3 (MeV)
-60
-40
-20
(a)
208Pb (16O, 12Cα) 150 MeV
300
200
100
Q3
(b)
9.84
10.35
11.09
11.52
30
20
10
E12 (g.s.)
(c)
30
20
10
E12 (DI)
2
4
6
E12 (MeV)

Fig. 4

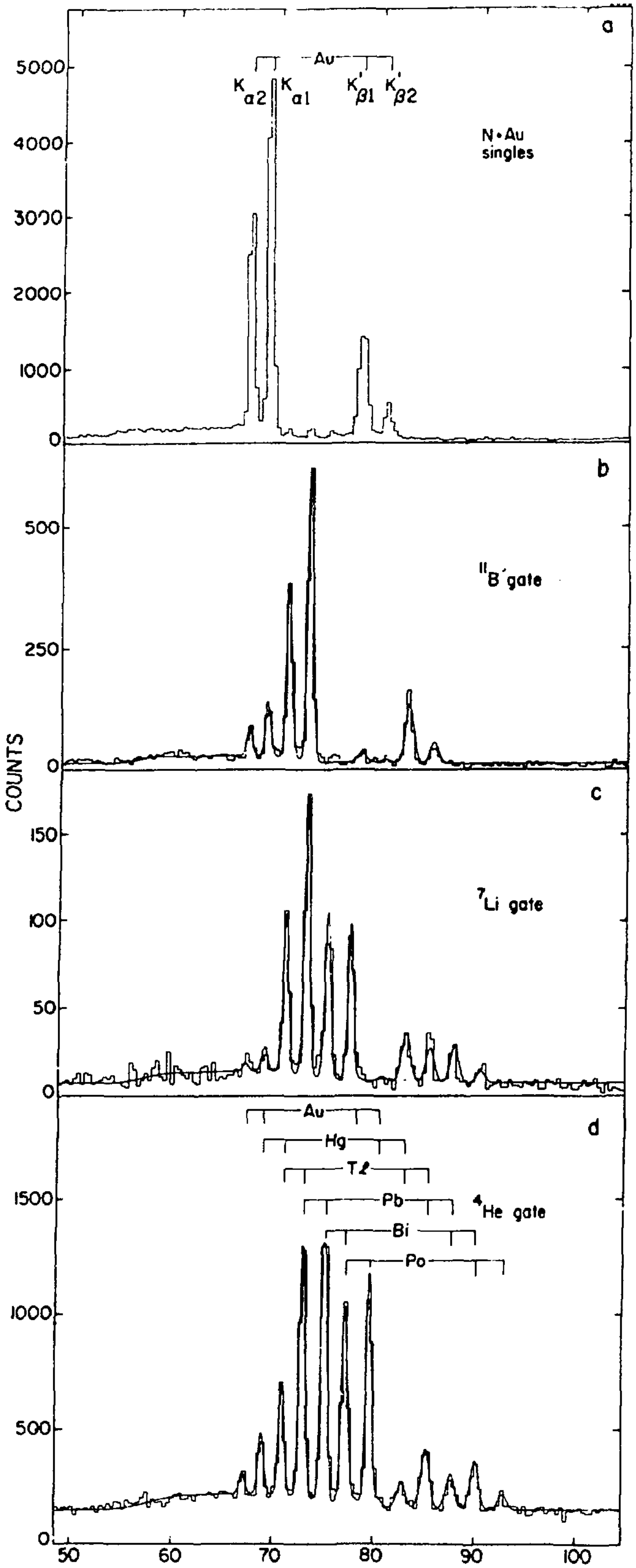
a
Au
$K_{\alpha 2}$ $K_{\alpha 1}$ $K'_{\beta 1}$ $K'_{\beta 2}$
N + Au
singles
b
^{11}B gate
c
^{7}Li gate
d
Au
Hg
Tl
Pb
Bi
Po
^{4}He gate
COUNTS
keV
0
1000
2000
3000
4000
5000
250
500
50
100
150
1500
60
70
80
90

Fig. 5

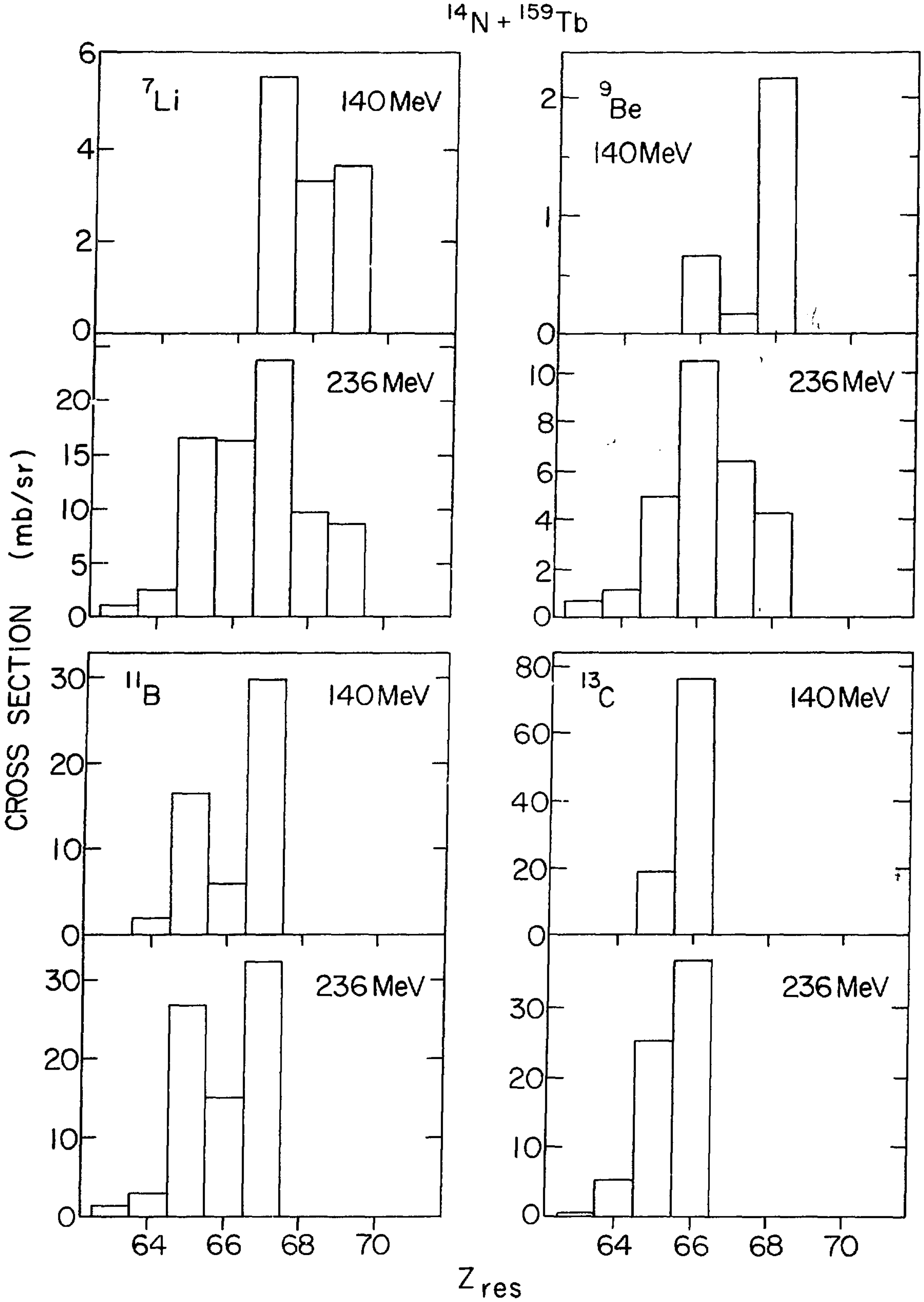

^{14}N + ^{159}Tb
^{7}Li
140 MeV
236 MeV
^{9}Be
140 MeV
236 MeV
^{11}B
140 MeV
236 MeV
^{13}C
140 MeV
236 MeV
CROSS SECTION (mb/sr)
Z res
64
66
68
70

Fig. 6

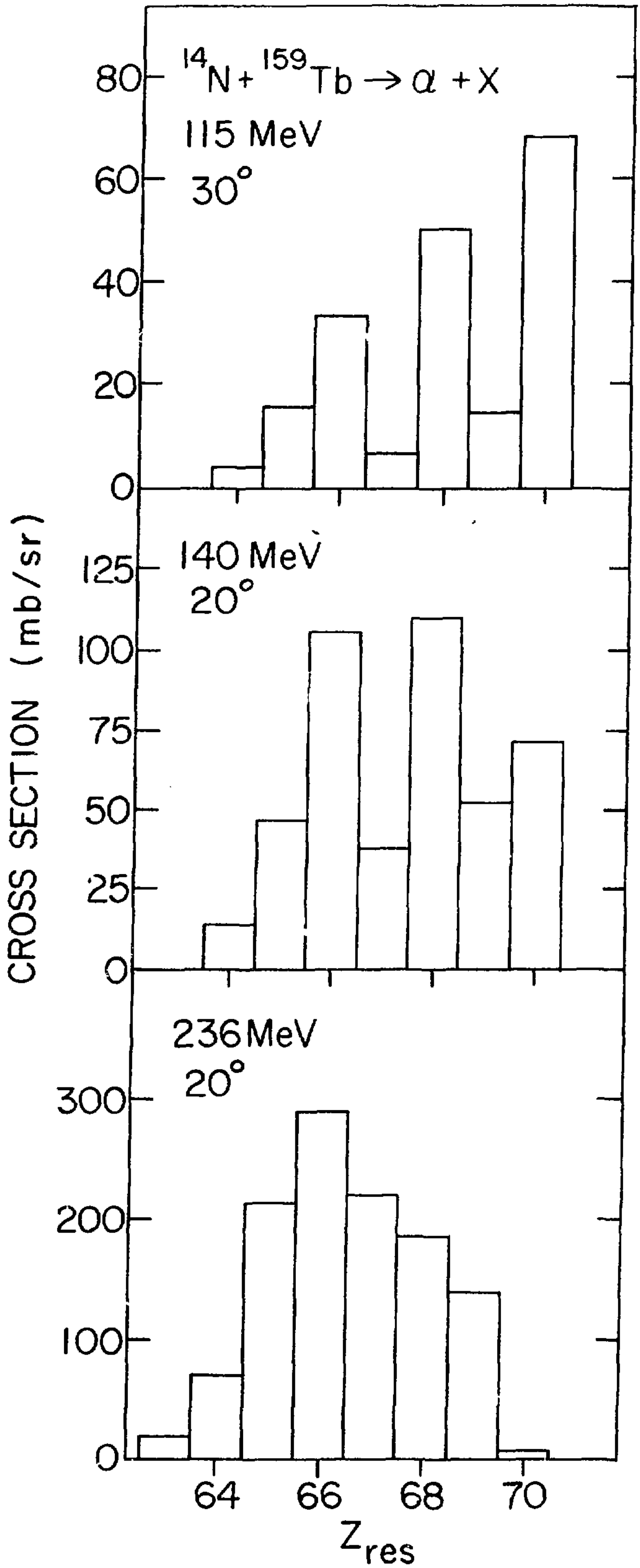
14N + 159Tb → α + X
115 MeV
30°
140 MeV
20°
236 MeV
20°
CROSS SECTION (mb/sr)
80
60
40
20
0
125
100
75
50
25
0
300
200
100
0
64
66
68
70
Zres

Fig. 7

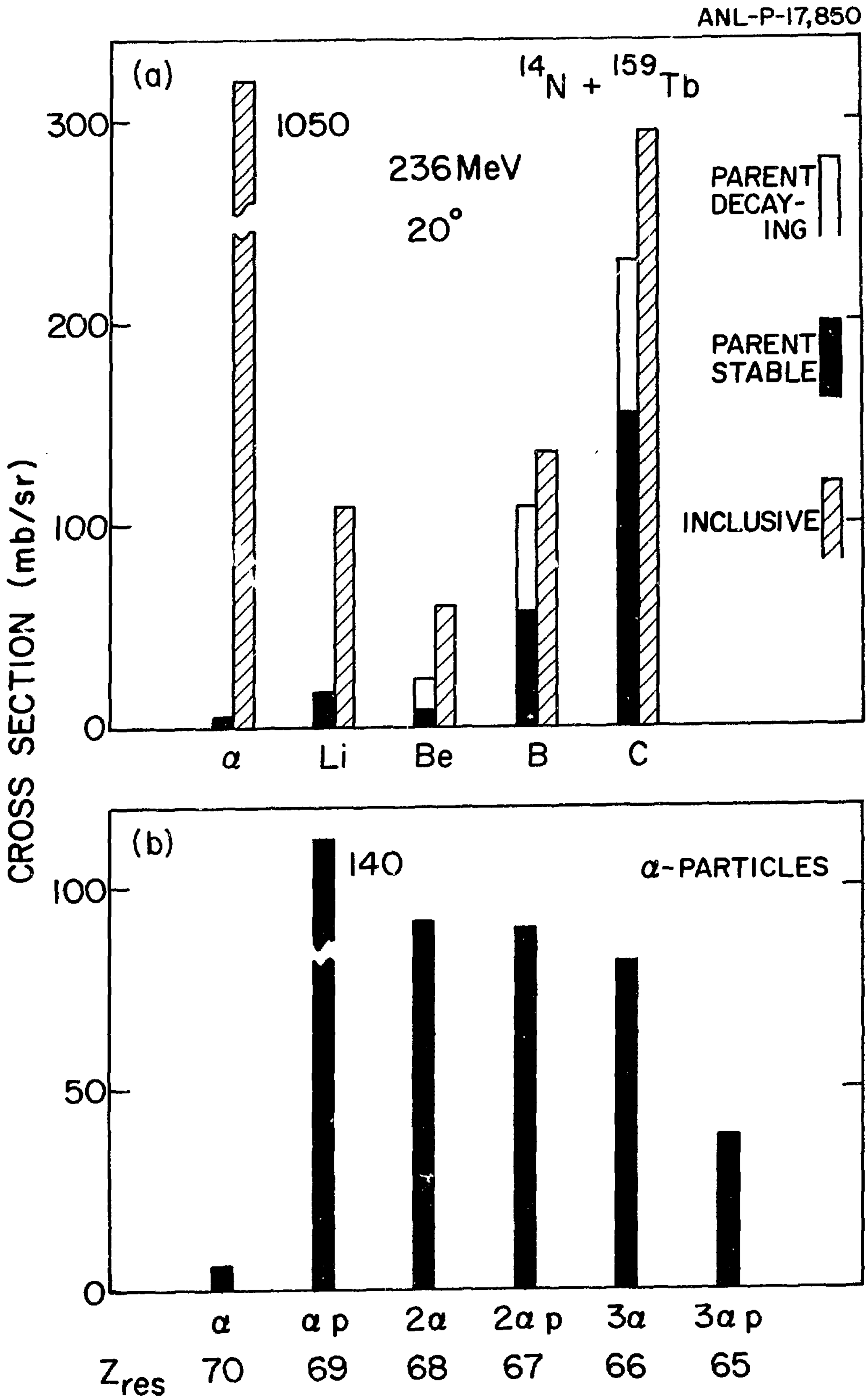
ANL-P-17,850
(a)
$^{14}N + ^{159}Tb$
236 MeV
20°
1050
PARENT DECAY-ING
PARENT STABLE
INCLUSIVE
CROSS SECTION (mb/sr)
0
100
200
300
α
Li
Be
B
C
(b)
140
α-PARTICLES
0
50
100
α
α p
2α
2α p
3α
3α p
Z_{res}
70
69
68
67
66
65

Fig. 8

ANL-P-17,880

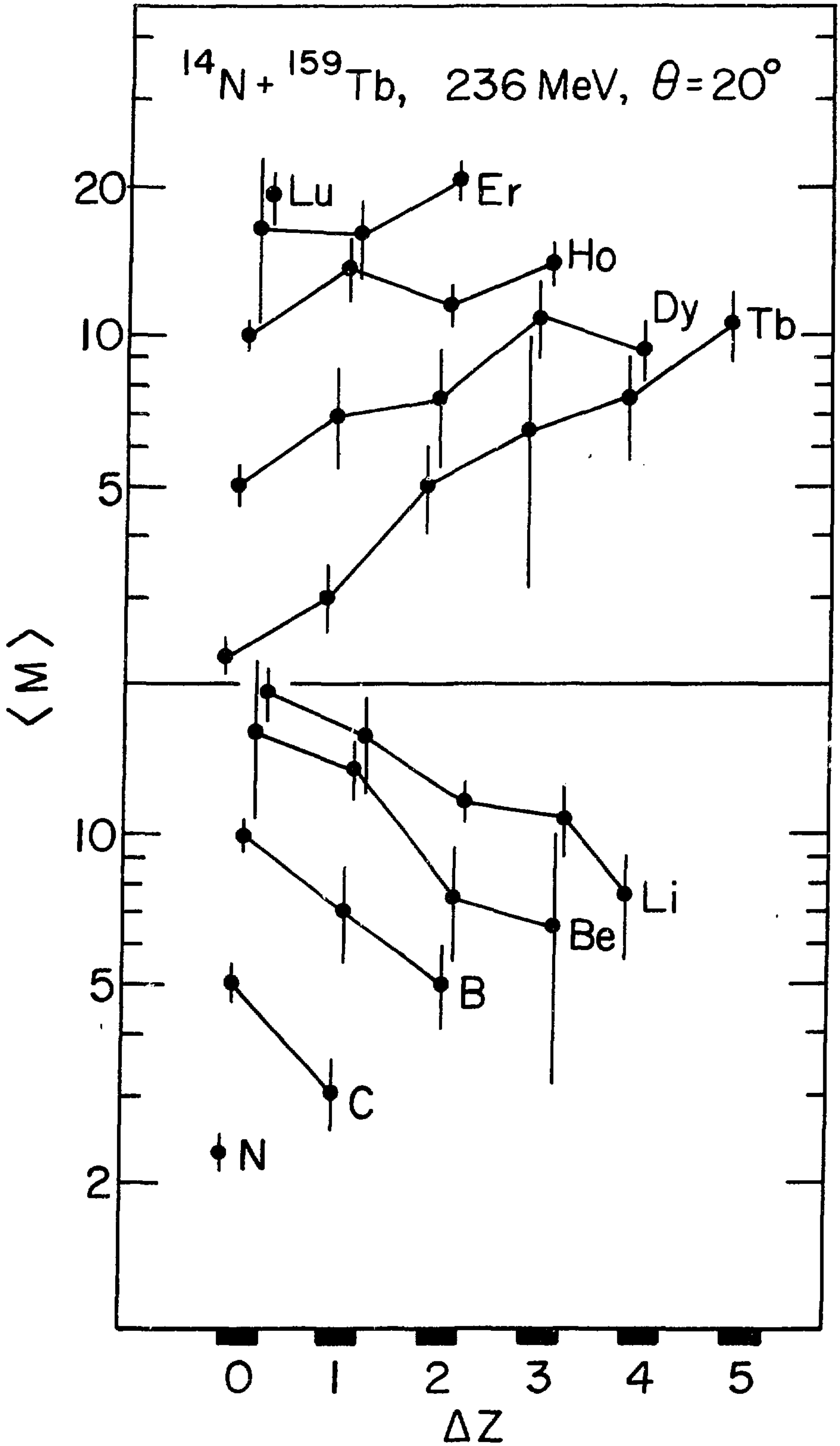

Fig. 9

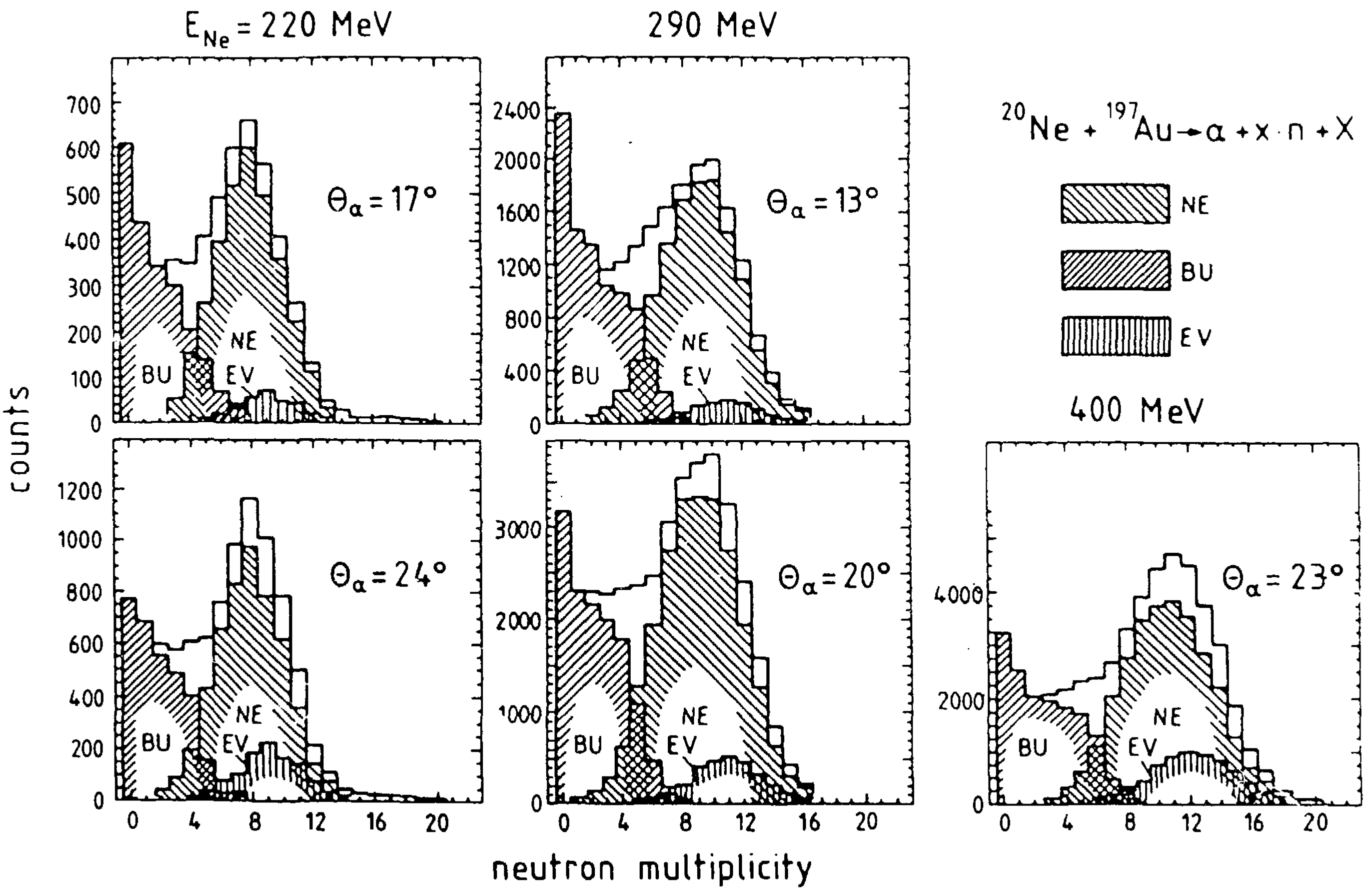

E_Ne = 220 MeV
290 MeV
400 MeV
20Ne + 197Au → α + x·n + X
NE
BU
EV
Θα = 17°
Θα = 13°
Θα = 24°
Θα = 20°
Θα = 23°
counts
neutron multiplicity

Fig. 10